ROYAL SOCIETY OF CHEMISTRY

Check for updates

All publication charges for this article have been paid for by the Royal Society of Chemistry

A structural reorganization-based catalytic hairpin assembly enabling small-molecule monitoring in living cells

Rui-Wen Wang,†[a] Wei-Guo Yang,†[a] Ming-Li Su,[a] Jia-Min Qin,[a] Jia-Qi Liu,[c] Xiao-Han Yang,[a] Jun-Yi Cao,[a] Ruo Yuan, [a] Ying Zhuo, *[a] Ming Chen, *[c] Chaoyong Yang *[b] and Wen-Bin Liang *[a]

Small-molecule drugs, constituting over 60% of FDA-approved therapeutics (2017–2022), present unresolved challenges relating to elucidating their intracellular mechanisms. We present a dual-strategy platform integrating "*in silico* aptamer affinity maturation" (ISAAM) and "structural reorganization-catalytic hairpin assembly" (SR-CHA). ISAAM computationally designs high-affinity aptamers, while SR-CHA eliminates undesired signals *via* energy-minimized conformational control, achieving a signal-to-background improvement over conventional CHA. This system enables ultrasensitive small-molecule monitoring in live cells, resolving traditional challenges of false positives and inefficiency. Demonstrated through intracellular imaging and kinetic studies, SR-CHA offers a robust tool for probing small-molecule interactions in biological systems, advancing drug discovery and diagnostic applications.

Introduction

Small molecules are ubiquitous in nature as basic units playing important constituent and regulatory roles in living systems.[1–3] Meanwhile, numerous synthetic small molecules are used as drugs to regulate life processes *via* adaptable routes. More than 60% of new chemical entities approved by the US Food and Drug Administration (FDA) are small-molecule drugs (2017–2022).[4] Small molecules are expected to drive innovation in future drug discovery, giving great significance to exploring the biological mechanisms of small molecules *in vivo*.[5–8] However, the biological mechanisms of most small molecules are still in doubt, which primarily stems from three key factors: first, conventional detection methodologies for small molecules frequently necessitate harsh reaction conditions; second, achieving specific molecular recognition and efficient signal transduction presents significant technical challenges; and third, the majority of small molecules cannot function as enzymatic substrates or participate in enzyme-associated reaction pathways. For instance, chloramphenicol (CAP) is a highly effective broad-spectrum antibiotic with strong inhibitory effects against both Gram-positive and Gram-negative bacteria, as confirmed by *in vitro* bacteriostatic tests and extensive clinical trials and applications.[9] Nevertheless, CAP with enormous toxic effects could readily accumulate in animals and humans, and may cause irreversible myelosuppressive reactions leading to aplastic anaemia.[10–12] While high-performance liquid chromatography (HPLC), liquid chromatography-tandem mass spectrometry (LC-MS), and paper-based antibiotic sensors (PAS) have demonstrated significant analytical advantages for CAP detection,[13–16] substantial technical challenges persist in developing reliable methods for monitoring CAP in living cellular systems. Consequently, accurately and sensitively monitoring the intracellular concentration and distribution of CAP remains a significant challenge, hindering the elucidation of its underlying biological mechanisms.[17] These limitations underscore the urgent need for detection methodologies that combine target specificity with intracellular environmental adaptability.

To address this demand, aptamer-based strategies show unique advantages and potential in the field of bioanalytical chemistry of small molecules. Their inherent target-recognition specificity and structural programmability can convert small-molecule recognition into nucleic acid structural information, generating a great deal of application value in the specific and sensitive analysis of small molecules.[16,18–20] However, current aptamer selection methodology exhibits

a Key Laboratory of Luminescence Analysis and Molecular Sensing (Southwest University), Ministry of Education, Institute of Developmental Biology and Regenerative Medicine, College of Chemistry and Chemical Engineering, Southwest University, Chongqing 400715, P. R. China. E-mail: wenbinliangasu@gmail.com

b Institute of Molecular Medicine, Shanghai Key Laboratory for Nucleic Acid Chemistry and Nanomedicine, State Key Laboratory of Oncogenes and Related Genes, School of Medicine, Shanghai Jiao Tong University, Shanghai, 200127, China. E-mail: cyyang@xmu.edu.cn

c Department of Clinical Laboratory Medicine, Southwest Hospital, Third Military Medical University (Army Medical University), Chongqing 400038, China. E-mail: chming1971@126.com

† These authors contributed equally to this work.

notable limitations in its flexibility. A significant challenge lies in developing stringent screening processes to identify specific aptamers from combinatorial libraries containing approximately 10^{14} to 10^{15} distinct molecular species.[21,22] To illustrate this limitation quantitatively, using the selection of a 40-nucleotide aptamer as a representative case, there are 4 (ref. 40) different sequences, making the probability of selecting the optimal one approximately 1 in 10^9, which is remarkably low, being several orders of magnitude smaller than winning a typical lottery jackpot. While increasing the library capacity presents a theoretically feasible approach for enhancing the probability of identifying optimal aptamers, the associated temporal and resource requirements render this strategy practically unsustainable. Conversely, in the case of small-molecule-targeting aptamers, the design parameters for nucleic acid conformational modifications are significantly constrained by the limited availability of binding sites. This restriction presents a substantial challenge in achieving an optimal equilibrium between binding affinity and structural stability.[23–26] Furthermore, nucleic acid structures with compromised stability may result in elevated background signal interference, thereby potentially compromising the reliability of detection systems. To completely exploit small-molecule binding sites, we propose the *in silico* aptamer affinity maturation (ISAAM) method, which analyzes the binding modes of small-molecule parent compounds with aptamers and provides guidance for aptamer design. Recently, we investigated the structures and interactions of HBC aptamers as artificial aptamers.[27] This provides the basis for the design of artificial aptamer affinity maturation, which is expected to yield high-affinity aptamers through design and reconstruction based on existing small-molecule aptamers obtained through screening.

In addition, efficient signal amplification strategies are indispensable for high-sensitivity analyses, particularly for small molecules exhibiting low binding energies to their aptamers. Catalytic hairpin assembly (CHA),[28–32] an enzyme-free nucleic acid amplification technique, employs toehold-mediated strand displacement (TMSD) under mild reaction conditions,[22,33,34] to achieve a theoretically predicted 10^6-fold acceleration in chain displacement kinetics, thereby establishing itself as a preeminent methodology in aptamer-mediated signal recognition-conversion systems. However, the obvious inherent flaws in the CHA strategy cannot be ignored. Even in the absence of an elicitation chain, the hairpins in the CHA circuit may react non-specifically, reducing the signal-to-background ratio (SBR) significantly.[35–37] Although several strategies, including mismatch-based approaches[35,38,39] have been developed to mitigate CHA signal leakage, the incorporation of such modifications often compromises reaction efficiency and specificity. Significant challenges remain in developing CHA systems that simultaneously achieve low background noise and high efficiency for reliable *in vivo* small-molecule detection.[40]

To address these challenges, we developed a small-molecule-triggered structural reorganization-CHA (SR-CHA) system, enabling the precise monitoring of CAP in both living cells and *in vitro* environments (Fig. 1). This integrated approach combines two key innovations. First, ISAAM-based aptamer augmentation technology enables high-affinity small-molecule recognition through molecule-nucleic acid sequence conversion. Additionally, the nucleic acid SR-CHA amplification strategy addresses signal-to-background ratio (SBR) limitations by minimizing unintended binding. The SR-CHA method demonstrates significant advantages in intracellular small-molecule analysis, offering reduced background interference compared to conventional CHA systems while maintaining high efficiency under physiological conditions. This advancement provides a robust platform for investigating CAP's intracellular mechanisms and distribution patterns.

Results and discussion

Aptamer optimization based on the ISAAM method

Starting from aptamer 0 (Fig. 2A), a known aptamer of CAP,[41,42] the number of bases bound to its stem was adjusted to increase the stability of the aptamer. A schematic diagram of the thermodynamic states of different structures of the aptamer is shown in Fig. 2F. The thermodynamic stability of the aptamer system is primarily governed by ΔG_2, which originates from the stem base-pairing energy. To minimize background signals resulting from spontaneous transitions to the linear state, the absolute value of ΔG_2 must be sufficiently large relative to ΔG_1. Simultaneously, structural modifications must preserve the integrity of the CAP binding site. Guided by these thermodynamic principles and structural considerations, we engineered three optimized aptamer variants through targeted base substitutions in non-CAP binding regions: (1) aptamer 1 (Fig. 2B) with a G11C substitution, (2) aptamer 2 (Fig. 2C) with a T13A substitution, and (3) aptamer 3 (Fig. 2D) containing both G11C and T13A substitutions.

These modifications achieved dual objectives: reducing structural-instability-induced signal leakage and increasing binding-site accessibility. Quantitative analysis of the thermodynamic stability revealed enhanced free-energy values for all optimized aptamers, as demonstrated in Fig. 2K. When CAP binds to the aptamer, the small-molecule interaction results in a structural shift of the aptamer, exposing the 16G to 27G region (REF) and triggering the subsequent CHA reaction. To investigate the ability of the four aptamers to release the REF portion upon binding to CAP, the REF portion of the aptamer was deleted, and the remaining portion (the CAP reaction domain) was used to dock to CAP; the results of the docking are shown in Fig. 2G–J. It can be seen in Fig. 2I and J that the remaining portions of aptamers 2 and 3 bind to CAP with a large change in chain morphology, forming a binding domain capable of encapsulating CAP. Furthermore, we analysed CAP-aptamer binding energies *via* Autodock 4 and aptamer-specific Gibbs free energies using the NUPACK webserver. The binding energy of aptamer 2 to CAP reached -7.37 kcal mol^{-1}, which is significantly better than the other three aptamers (Fig. 2K). Considering the stability of the aptamer and the magnitude of binding energy to the target small molecules, aptamer 2 has superior performance at present.
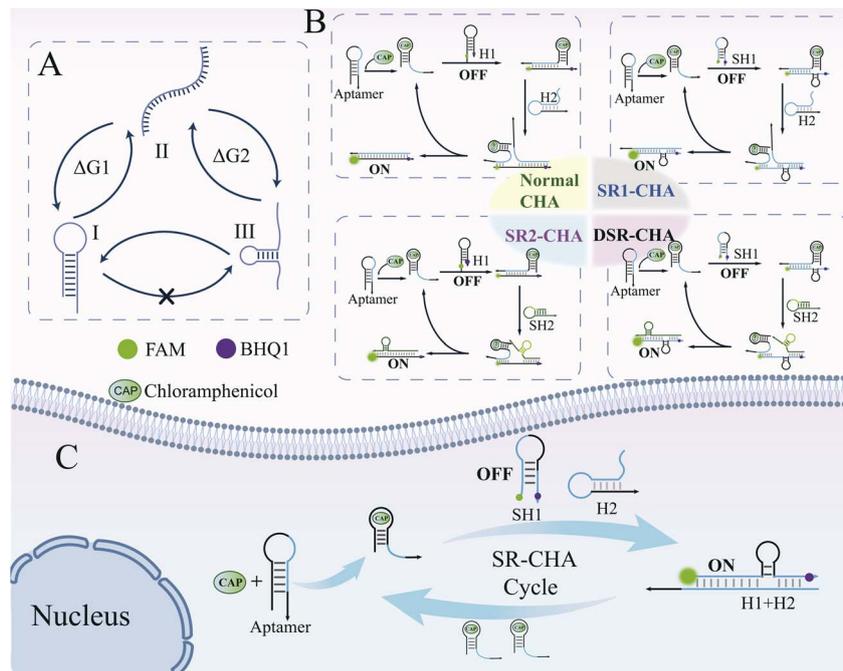
Fig. 1 Schematic diagrams of small-molecule-initiated SR-CHA for the amplified detection of CAP. (A) A schematic diagram of the transformation of nucleic acid chains with different structures. (B) A schematic diagram of the cyclic process of small-molecule-initiated normal CHA and SR-CHAs. (C) The intracellular SR1-CHA cycle process.

Under the optimized conditions (Fig. S3), the superior performance of aptamer 2 was further confirmed by fluorescence experiments (Fig. 2L). As can be seen in the figure, aptamer 2 was able to achieve a significantly enhanced signal above the background value. Aptamer 2 was selected for all subsequent experiments based on its superior binding affinity and stability compared to the other candidates.

Thermodynamic models and thermodynamic analysis of SR-CHA and conventional CHA

To elucidate the mechanistic details and intermediate states associated with branch migration in SR-CHA systems, we conducted comparative thermodynamic analysis between SR-CHA and conventional CHA. Toehold-mediated strand displacement (TMSD) is a fundamental nucleic acid reaction process in which a single-stranded (ss) nucleic acid invader strand initiates binding at a terminal overhang region (toehold) of a double-stranded DNA (dsDNA) complex, subsequently displacing the incumbent strand through a branch migration mechanism (Fig. 3A).[43] Srinivas *et al.*[44] built a thermodynamic model for a TMSD process (Fig. 3B). They modelled branch migration at a detailed level that explicitly includes intermediates, thereby highlighting important thermodynamic features of the process that are not evident from a phenomenological approach.

On the basis of this thermodynamic model, we can analyse the thermodynamic processes of structural CHA and normal CHA. For all four CHA processes mentioned above, the first step is to bind to CAP and then deform the aptamer to expose the part that triggers the next step of CHA. Here, to simplify the representation, we omit the deformation step and directly represent the trigger chain with the blue part shown in the figures. For the conventional CHA process, the trigger first binds to the toehold of H1, after which it opens the stem of the H1 hairpin to form the H1-trigger complex; next, H2 binds to the toehold of H1, displacing the trigger and allowing the cycle to continue. The thermodynamic changes of this process are shown in Fig. 3C, and all specific values of free energy (G) in the figures are from NUPACK. However, in the thermodynamic process of SR1-CHA, as depicted in Fig. 3D, the binding of the trigger induces the structural reorganization of SH1 to form a structural-reorganization work unit (SWU). The interaction between reconfigured SH1 and the trigger exhibits a lower ΔG, which significantly mitigates signal leakage associated with the CHA process. Afterwards, H2 binds to the SH1-trigger complex and releases the trigger, allowing the trigger to continue the cycle.

This reduction in ΔG enhances the thermodynamic stability of the system, thereby improving the overall fidelity and efficiency of the reaction. In the SR2-CHA system (Fig. 3E), while the H1 hairpin maintained its structural integrity, the SH2 component exhibited conformational rearrangement upon recognizing the toehold binding region of the H1-trigger complex, resulting in the formation of a stable SWU structure. This structural reorganization induced a substantial decrease in the ΔG of the system, thereby enhancing its thermodynamic stability. Subsequently, SH2 fully binds to H1, releasing the trigger to re-enter the CHA cycle, thereby enabling continuous signal amplification and improving the efficiency of the reaction. Through the strategic integration of SR1-CHA and SR2-
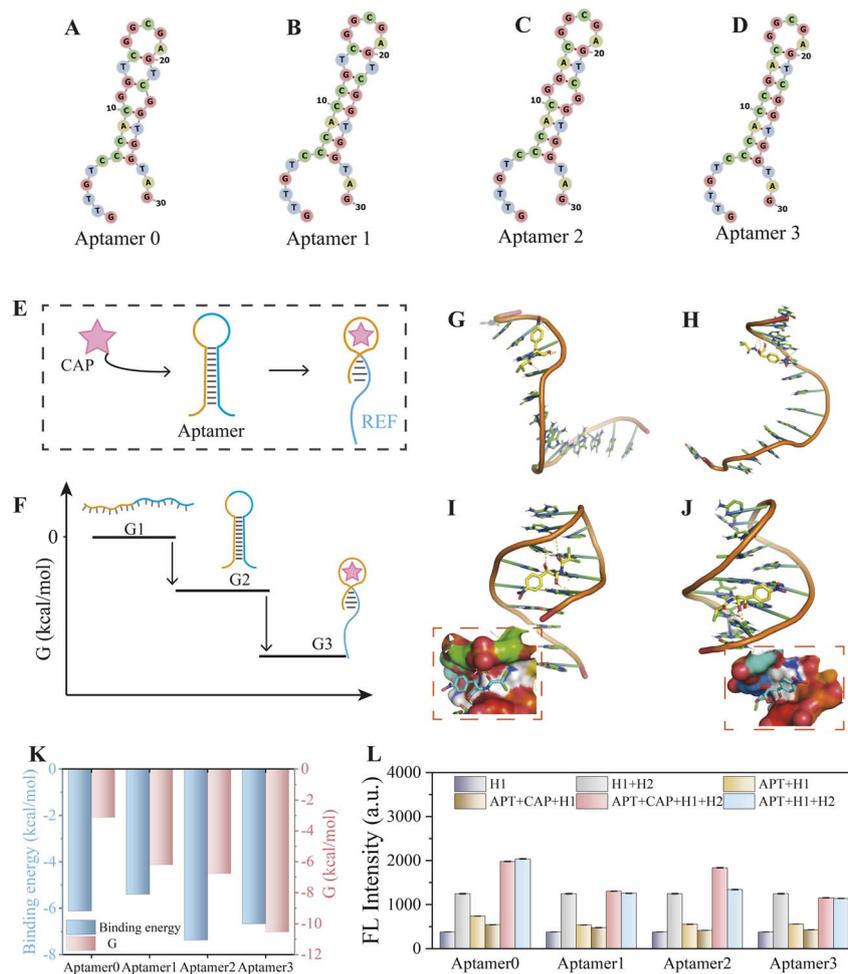
Fig. 2 The initial CAP aptamer, aptamer 0 (A); replacing its 11G base with C gave aptamer 1 (B), replacing its 13T base with A gave aptamer 2 (C), and changing both 11G and 13T gave aptamer 3 (D). (E) A schematic diagram of the conformational change that occurs when the aptamer binds to CAP. (F) Energy changes during conformational transitions of the aptamer. (G–J) Results of docking with CAP after the removal of the REF part of each aptamer, showing the docking domain with CAP. (K) Binding energies of aptamers 0, 1, 2, and 3 from CAP docking and the free energy (G) of each aptamer. (L) Fluorescence experiments with the four aptamers with 500 nM CAP.

CHA mechanisms, we developed a dual-structural reorganization CHA (DSR-CHA) system that incorporates two metastable structural transformation processes. This design integrates two sequential metastable structural transitions that cooperatively suppress undesired background signals through energy landscape optimization, theoretically enabling better background-reduction efficiency compared to conventional CHA systems, as shown in Fig. 3F.

Kinetic analysis of small-molecule-induced SR-CHA and normal CHA

Real-time fluorescence experiments were further employed to investigate the kinetic characteristics of SR-CHA. As shown in Fig. 4A, non-fluorescent-labelled strands were first introduced into cuvettes and then excited at 497 nm for 600 s. As no fluorescent strands were present, this period established both a near-zero baseline and a zero-background signal for the first 600 s. At precisely 600 s, fluorescent-labeled strands were simultaneously introduced to all reaction systems. This protocol ensured quantitatively comparable initial signal levels between CAP-positive and CAP-negative groups during real-time fluorescence monitoring, thus preventing signal discrepancies arising from baseline inconsistencies. Upon the introduction of H1, which was labelled with FAM and BHQ1, a gradual increase in fluorescence signal was observed following the establishment of a stable baseline. The fluorescence intensity at an emission wavelength of 520 nm was monitored in real time over a period of 6000 s. Fig. 4B–E shows the kinetic performances of normal CHA, SR1-CHA, SR2-CHA and DSR-CHA, respectively. In the conventional CHA system, the introduction of CAP induces a significant enhancement in fluorescence intensity compared to the CAP-free control, with the signal reaching saturation after approximately 4000 s. Beyond this time point, the fluorescence intensity stabilizes, exhibiting no further temporal increase, and a constant $(F - F_0)/F_0$ ratio is maintained. For SR1-CHA, the fluorescence signal is weaker and increases more slowly compared to normal CHA. However, in Fig. 4C, the fluorescence signal of the CAP-positive group continues to rise at 6000 s,
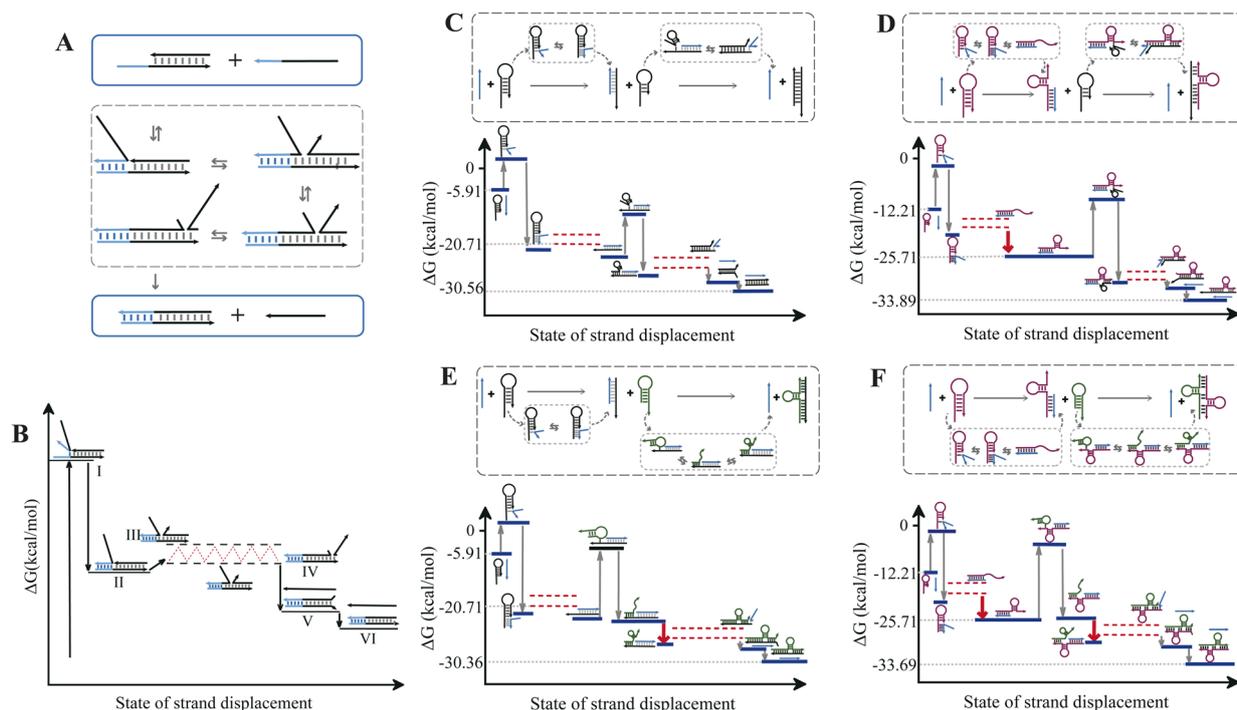
Fig. 3 (A) A schematic illustration of a toehold-mediated strand displacement process. (B) Free-energy modelling of a toehold-mediated strand displacement process. (C–F) The processes of free-energy changes in different steps for normal CHA (C), SR1-CHA (D), SR2-CHA (E) and DSR-CHA (F).

whereas the background signal stabilizes earlier. In this regard, it can be hypothesized that the kinetic response of the reaction is slowed down due to the metathesis process of SH1, but SR1-CHA shows superior kinetic potential. Compared to

conventional CHA, SR1-CHA also exhibited higher $(F - F_0)/F_0$ values, further demonstrating its capacity to reduce the CHA response background. SR2-CHA demonstrated a much faster response compared to normal CHA, reaching a stable high
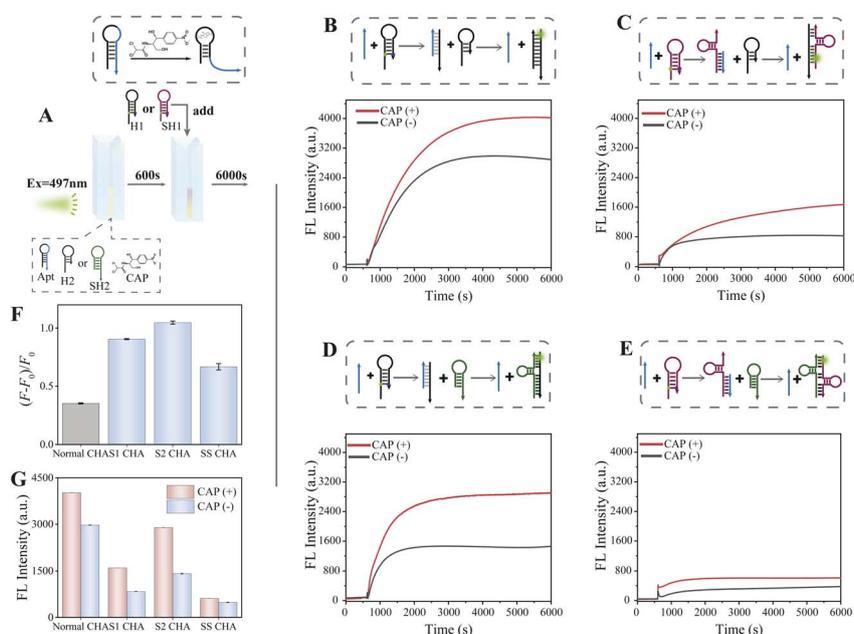

Fig. 4 (A) A schematic diagram of the kinetic experiment process. Dynamic fluorescence signals of (B) normal CHA, (C) SR1-CHA, (D) SR2-CHA and (E) DSR-CHA over 6000 s at 37 °C. (F) A comparison of the $(F - F_0)/F_0$ values for the four CHA systems. (G) CAP-negative and -positive fluorescence signal values for the four CHA systems after hybridization at 37 °C for 2 h.

signal value within about 2500 s, while the $(F - F_0)/F_0$ value of the response was significantly better than that of normal CHA. As predicted previously for the reaction, DSR-CHA exhibits extremely slow kinetics, and even after a reaction time of 6000 s, fluorescence signal growth is barely visible; although it reaches a higher $(F - F_0)/F_0$ value, the overall signal remains low.

From a kinetic analysis of the four CHA systems, distinct reaction characteristics were observed. In SR1-CHA, the structural reorganization primarily occurs at SH1, resulting in relatively slower reaction kinetics. Although the fluorescence intensity achieved within 6000 s is limited, this system demonstrates considerable reaction potential, suggesting that an extended reaction duration could yield improved $(F - F_0)/F_0$ values. In contrast, SR2-CHA exhibits superior kinetic performance due to its partial structural reorganization at SH2, which not only maintains the reaction velocity but also demonstrates enhanced background suppression. Although theoretical predictions suggested that the DSR-CHA system could exhibit optimal reaction performance, its kinetic efficiency is substantially limited by the concurrent structural reorganization processes required at both SH1 and SH2 domains. This dual-site conformational rearrangement introduces thermodynamic barriers that impede the progression of the catalytic reaction.

A performance comparison of conventional CHA and SR-CHA in CAP analysis

Under the optimal conditions, the performance of the proposed SR-CHA for the detection of CAP was examined (Fig. S9A–D). Different concentrations of CAP were detected with the four CHA detection systems. It was observed that the fluorescence intensity exhibited a gradual increase as the concentration of CAP was changed from 1 pM to 100 nM (Fig. S9E–H). As demonstrated in Fig. S9I–L, for all four CHA systems, there was an increase in the $(F - F_0)/F_0$ ratio with a rise in the concentration of CAP; the ratio was linearly associated with $\lg c_{CAP}$ in the range of 1 pM to 100 nM, and showed linearity in the detection of CAP. The Pearson correlation coefficients (r) for SR1-CHA and SR2-CHA were calculated to be 0.9918 and 0.9932, respectively, exceeding that of conventional CHA ($r = 0.9565$), which demonstrates that the SR-CHA system exhibits superior linearity in CAP detection compared to its conventional counterpart. Furthermore, SR1-CHA and SR2-CHA can achieve higher $(F - F_0)/F_0$ ratios with 2.5–3 times higher sensitivity, which implies that our proposed SR-CHA has a better detection performance. Additionally, practical validation using real samples (honey and milk) also yielded robust detection results, as illustrated in Fig. S10. These results suggest that the SR-CHA strategy has great potential for application to CAP analysis in
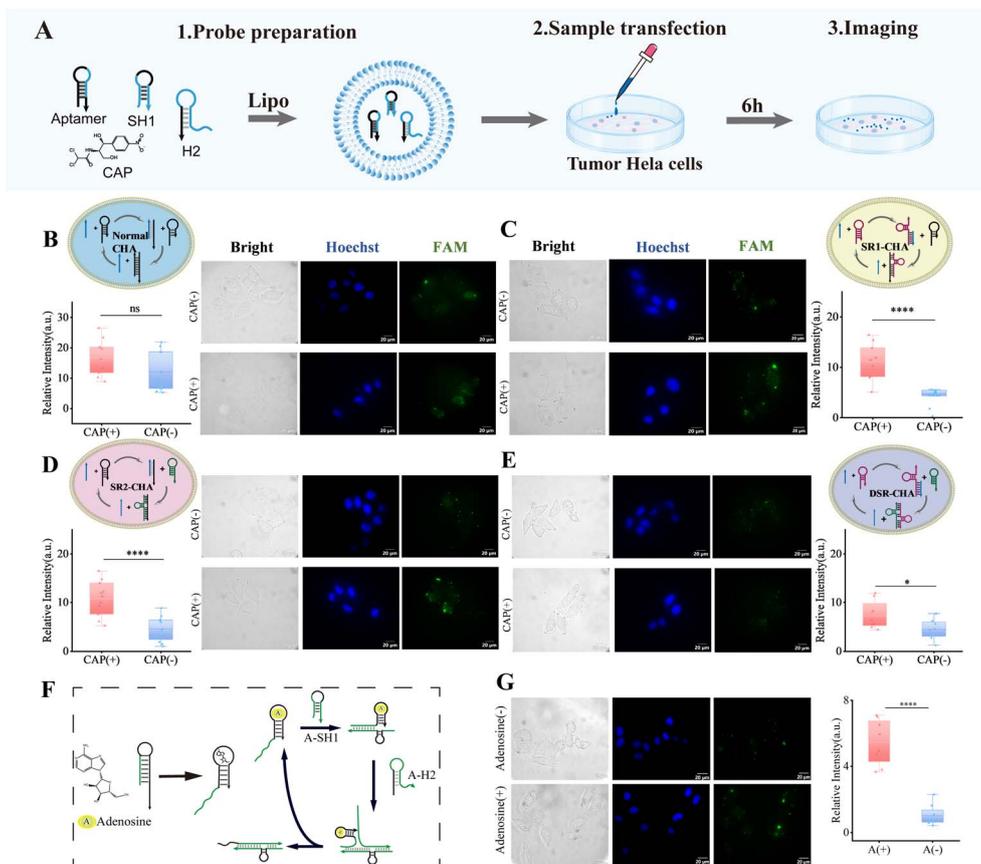

Fig. 5 (A) A schematic diagram of the intracellular imaging steps. Fluorescence imaging of normal CHA (B), SR1-CHA (C), SR2-CHA (D) and DSR-CHA (E) in HeLa cells. (F) A schematic diagram of the adenosine-mediated SR1-CHA process. (G) The fluorescence imaging of SR1-CHA to detect adenosine intracellularly.

real samples. It is noteworthy that the $(F - F_0)/F_0$ ratio exhibited by DSR-CHA is found to approximate that of regular CHA, a result that is rather unexpected. However, this phenomenon suggests that for DSR-CHA, although the background can be effectively reduced to a certain extent, kinetic effects during the reaction should not be neglected. The formation of two SWUs by SH1 and SH2 in DSR-CHA leads to reduced sensitivity in the detection of small molecules, and a longer reaction time may be necessary for sensitive analysis.

Small-molecule imaging in living cells based on conventional CHA and SR-CHA

To explore the intracellular expression of structural SR-CHA, we fluorescently imaged conventional CHA and the three SR-CHA systems in cervical cancer (HeLa) cells. The behaviour of the four CHA systems in HeLa cells was consistent with the fluorescence signals measured *in vitro*. In the traditional CHA system (Fig. 5B), while the CAP-containing experimental group generated somewhat higher FAM signals than the blank group, the blank controls themselves showed significant background interference. For structural SR1-CHA (Fig. 5C) and SR2-CHA (Fig. 5D), after setting up experimental groups with CAP and blank groups with TE buffer instead of CAP, both experimental groups produced FAM fluorescence signals significantly higher than the background. However, for DSR-CHA (Fig. 5E), which is also a structural reorganization-based CHA, both experimental and control groups triggered only low fluorescence signals, and there was no obvious difference in signal intensity between the experimental and control groups. The intracellular imaging experiments illustrate that the SR-CHA strategy is not only suitable for *in vitro* assays but also has potential for intracellular assays. This highlights the versatility and broad applicability of the SR-CHA strategy, paving the way for its future use in complex biological systems and clinical diagnostics.

Application of the SR-CHA strategy to the detection of adenosine molecules

In order to demonstrate the general applicability of the SR-CHA strategy and expand its scope of application, we redesigned the SR1-CHA cycle using adenosine (A) molecules as targets and evaluated the performance of this reaction. A schematic diagram of the SR1-CHA system mediated with adenosine is shown in Fig. 5F, in which the detection performance of the CHA system showed promising results, both in terms of selectivity and linearity (Fig. S11). In addition, we also performed intracellular fluorescence imaging experiments and found that adenosine-mediated SR1-CHA also effectively detected adenosine in cells. As shown in Fig. 5G, the positive fluorescence imaging results for intracellular adenosine significantly diverged from the negative fluorescence imaging results, which confirms the universality of our proposed SR-CHA strategy. Therefore, we anticipate that through rational sequence design tailored to specific small molecules, an efficient detection strategy with minimal background interference can be developed. This approach holds significant potential for both *in vivo*

and *in vitro* applications, enabling the highly sensitive and specific detection of small molecules.

Conclusions

In conclusion, we have established a novel SR-CHA strategy for sensitive small-molecule detection. The enhanced performance of this approach was systematically validated through comprehensive fluorescence assays, kinetic studies, thermodynamic characterization, and intracellular imaging studies. Comparative analysis with a conventional CHA system revealed the distinct advantages of the SR-CHA strategy. The SR-CHA strategy demonstrates three significant advantages over conventional CHA systems: (1) enhanced molecular specificity and detection sensitivity for small-molecule targets, (2) a substantially reduced background signal through the elimination of self-hybridization artifacts characteristic of traditional two-strand CHA systems, and (3) improved cellular imaging capabilities coupled with superior circuit efficiency in biological environments. We envision that this innovative strategy will provide a versatile platform for advanced biosensing applications, enabling fundamental *in vivo* bioanalytical research. It also facilitates mechanistic investigations of small-molecule interactions at the cellular level.

Author contributions

R. W., and W. Y. contributed equally to this work. W. L. designed the research; R. W., W. Y., and J. Q., performed the research; R. W., W. Y., M. S., J. L., X. Y., J. C., and R. Y., analysed data; W. L., Y. Z., M. C., and C. Y., supervised the work; R. W., W. Y. and W. L. wrote the paper. All authors read and approved the final manuscript.

Conflicts of interest

There are no conflicts to declare.

Data availability

The data supporting this article have been included as part of the SI.

Supplementary information: Nucleic acid sequences, materials, reagents, apparatus and detailed experimental procedures. See DOI: **https://doi.org/10.1039/d5sc04624f**.

Acknowledgements

References

1 S. Qiu, Y. Cai, H. Yao, C. Lin, Y. Xie, S. Tang and A. Zhang, Small molecule metabolites: discovery of biomarkers and therapeutic targets, *Signal Transduct. Targeted Ther.*, 2023, **8**, 132.

2 S. Qiu, Y. Cai, Z. Wang, Y. Xie and A. Zhang, Decoding functional significance of small molecule metabolites, *Biomed. Pharmacother.*, 2023, **158**, 114188.

3 A. Gutteridge, M. Kanehisa and S. Goto, Regulation of metabolic networks by small molecule metabolites, *BMC Bioinf.*, 2007, **8**, 88.

4 P. Bhutani, G. Joshi, N. Raja, N. Bachhav, P. K. Rajanna, H. Bhutani, A. T. Paul and R. Kumar, U.S. FDA Approved Drugs from 2015-June 2020: A Perspective, *J. Med. Chem.*, 2021, **64**, 2339–2381.

5 L. M. Mustachio, A. Chelariu-Raicu, L. Szekvolgyi and J. Roszik, Targeting KRAS in Cancer: Promising Therapeutic Strategies, *Cancers*, 2021, **13**, 1204.

6 D. R. Owen, C. M. N. Allerton, A. S. Anderson, L. Aschenbrenner, M. Avery, S. Berritt, B. Boras, R. D. Cardin, A. Carlo, K. J. Coffman, A. Dantonio, L. Di, H. Eng, R. Ferre, K. S. Gajiwala, S. A. Gibson, S. E. Greasley, B. L. Hurst, E. P. Kadar, A. S. Kalgutkar, J. C. Lee, J. Lee, W. Liu, S. W. Mason, S. Noell, J. J. Novak, R. S. Obach, K. Ogilvie, N. C. Patel, M. Pettersson, D. K. Rai, M. R. Reese, M. F. Sammons, J. G. Sathish, R. S. P. Singh, C. M. Steppan, A. E. Stewart, J. B. Tuttle, L. Updyke, P. R. Verhoest, L. Wei, Q. Yang and Y. Zhu, An oral SARS-CoV-2 M(pro) inhibitor clinical candidate for the treatment of COVID-19, *Science*, 2021, **374**, 1586–1593.

7 M. Y. Fang, S. Markmiller, A. Q. Vu, A. Javaherian, W. E. Dowdle, P. Jolivet, P. J. Bushway, N. A. Castello, A. Baral, M. Y. Chan, J. W. Linsley, D. Linsley, M. Mercola, S. Finkbeiner, E. Lecuyer, J. W. Lewcock and G. W. Yeo, Small-Molecule Modulation of TDP-43 Recruitment to Stress Granules Prevents Persistent TDP-43 Accumulation in ALS/FTD, *Neuron*, 2019, **103**, 802–819.

8 J. Li, X. Yao, J. Ma, C. Liu, W. Hong, H. Wu, M. Li and L.-H. Guo, Recent advances in the electrochemiluminescence detection of small molecule drugs, *Analyst*, 2025, **150**, 1048–1065.

9 Y. Sun, G. I. N. Waterhouse, X. Qiao, J. Xiao and Z. Xu, Determination of chloramphenicol in food using nanomaterial-based electrochemical and optical sensors-A review, *Food Chem.*, 2023, **410**, 135434.

10 E. Nordkvist, T. Zuidema, R. G. Herbes and B. J. A. Berendsen, Occurrence of chloramphenicol in cereal straw in north-western Europe, *Food Addit. Contam.,:Part A*, 2016, **33**, 798–803.

11 H. Tsai, H. C. Hu, C. C. Hsieh, Y. H. Lu, C. H. Chen and C. B. Fuh, Fluorescence studies of the interaction between chloramphenicol and nitrogen-doped graphene quantum dots and determination of chloramphenicol in chicken feed, *J. Chin. Chem. Soc.*, 2019, **67**, 152–159.

12 S. Deng, F. Wang, Y. Li, J. Li, J. Zhan, Y. Shen, Z. Peng, C. Song, R. Cai, H. Yang and W. Tan, Triple Helix Molecular Switch Cascade Multiple Signal Amplification Strategies for Ultrasensitive Chloramphenicol Detection, *Anal. Chem.*, 2024, **96**, 20312–20317.

13 X. Wang, J. Li, D. Jian, Y. Zhang, Y. Shan, S. Wang and F. Liu, Paper-based antibiotic sensor (PAS) relying on colorimetric indirect competitive enzyme-linked immunosorbent assay for quantitative tetracycline and chloramphenicol detection, *Sens. Actuators, B*, 2021, **329**, 129173.

14 H. Kikuchi, T. Sakai, R. Teshima, S. Nemoto and H. Akiyama, Total determination of chloramphenicol residues in foods by liquid chromatography-tandem mass spectrometry, *Food Chem.*, 2017, **230**, 589–593.

15 H. N. Jung, D. H. Park, Y. J. Choi, S. H. Kang, H. J. Cho, J. M. Choi, J. H. Shim, A. A. Zaky, A. M. Abd El-Aty and H. C. Shin, Simultaneous Quantification of Chloramphenicol, Thiamphenicol, Florfenicol, and Florfenicol Amine in Animal and Aquaculture Products Using Liquid Chromatography-Tandem Mass Spectrometry, *Front. Nutr.*, 2021, **8**, 812803.

16 S. Wu, H. Zhang, Z. Shi, N. Duan, C. Fang, S. Dai and Z. Wang, Aptamer-based fluorescence biosensor for chloramphenicol determination using upconversion nanoparticles, *Food Control*, 2015, **50**, 597–604.

17 A. Yamagishi, F. Ito and C. Nakamura, Study on Cancer Cell Invasiveness via Application of Mechanical Force to Induce Chloride Ion Efflux, *Anal. Chem.*, 2021, **93**, 9032–9035.

18 A. Ruscito and M. C. DeRosa, Small-Molecule Binding Aptamers: Selection Strategies, Characterization, and Applications, *Front. Chem.*, 2016, **4**, 14.

19 A. K. Sharma and J. M. Heemstra, Small-Molecule-Dependent Split Aptamer Ligation, *J. Am. Chem. Soc.*, 2011, **133**, 12426–12429.

20 H. Yu, O. Alkhamis, J. Canoura, Y. Liu and Y. Xiao, Advances and Challenges in Small-Molecule DNA Aptamer Isolation, Characterization, and Sensor Development, *Angew. Chem., Int. Ed. Engl.*, 2021, **60**, 16800–16823.

21 X. Yang, C. H. Chan, S. Yao, H. Y. Chu, M. Lyu, Z. Chen, H. Xiao, Y. Ma, S. Yu, F. Li, J. Liu, L. Wang, Z. Zhang, B.-T. Zhang, L. Zhang, A. Lu, Y. Wang, G. Zhang and Y. Yu, DeepAptamer: advancing high-affinity aptamer discovery with a hybrid deep learning model, *Mol. Ther. Nucleic Acids*, 2025, **36**, 102436.

22 Y. Ding and J. Liu, Pushing Adenosine and ATP SELEX for DNA Aptamers with Nanomolar Affinity, *J. Am. Chem. Soc.*, 2023, **145**, 7540–7547.

23 Y. Zhang, L. Zhu, X. Ma, S. Zhu, Y. Ma, S. Hussain, X. He and W. Xu, An Effective Docking-Guided Strategy for Rational Tailoring of Fluorescent Aptamer Switches of Dimethylindole Red Analogue, *Anal. Chem.*, 2023, **95**, 7076–7081.

24 L. F. M. Passalacqua, M. R. Starich, K. A. Link, J. Wu, J. R. Knutson, N. Tjandra, S. R. Jaffrey and A. R. Ferré-D'Amaré, Co-crystal structures of the fluorogenic aptamer beetroot show that close homology may not predict similar RNA architecture, *Nat. Commun.*, 2023, **14**, 2969.

25 H. Chen, Y. Li, Z. Xiao, J. Li, T. Li, Z. Wang, Y. Liu and W. Tan, Chemical Amplification-Enabled Topological Modification of Nucleic Acid Aptamers for Enhanced Cancer-Targeted Theranostics, *ACS Nano*, 2023, **17**, 17740–17750.

26 R. Nutiu and Y. Li, In vitro Selection of Structure-Switching Signaling Aptamers, *Angew. Chem., Int. Ed.*, 2005, **44**, 1061–1065.

27 H.-R. Chen, M.-L. Su, Y.-M. Lei, Z.-X. Ye, Z.-P. Chen, P.-Y. Ma, R. Yuan, Y. Zhuo, C.-Y. Yang and W.-B. Liang, Insights of Life Molecules' Dynamic Distribution in Live Cells via Sequence–Structure Bispecific Fluorescent RNA, *J. Am. Chem. Soc.*, 2023, **145**, 12812–12822.

28 Z. Luo, Y. Li, P. Zhang, L. He, Y. Feng, Y. Feng, C. Qian, Y. Tian and Y. Duan, Catalytic hairpin assembly as cascade nucleic acid circuits for fluorescent biosensor: design, evolution and application, *TrAC, Trends Anal. Chem.*, 2022, **151**, 116582.

29 F. C. Simmel, B. Yurke and H. R. Singh, Principles and Applications of Nucleic Acid Strand Displacement Reactions, *Chem. Rev.*, 2019, **119**, 6326–6369.

30 Y. Si, L. Xu, T. Deng, J. Zheng and J. Li, Catalytic Hairpin Self-Assembly-Based SERS Sensor Array for the Simultaneous Measurement of Multiple Cancer-Associated miRNAs, *ACS Sens.*, 2020, **5**, 4009–4016.

31 F. Ma, C.-C. Li and C.-Y. Zhang, Nucleic acid amplification-integrated single-molecule fluorescence imaging for in vitro and in vivo biosensing, *Chem. Commun.*, 2021, **57**, 13415–13428.

32 C. A. Cox, A. N. Ogorek, J. P. Habumugisha and J. D. Martell, Switchable DNA Photocatalysts for Radical Polymerization Controlled by Chemical Stimuli, *J. Am. Chem. Soc.*, 2023, **145**, 1818–1825.

33 A. J. Genot, D. Y. Zhang, J. Bath and A. J. Turberfield, Remote Toehold: A Mechanism for Flexible Control of DNA Hybridization Kinetics, *J. Am. Chem. Soc.*, 2011, **133**, 2177–2182.

34 A. D. Ellington and J. W. Szostak, In vitro selection of RNA molecules that bind specific ligands, *Nature*, 1990, **346**, 818–822.

35 Y. S. Jiang, S. Bhadra, B. Li and A. D. Ellington, Mismatches improve the performance of strand-displacement nucleic acid circuits, *Angew. Chem., Int. Ed. Engl.*, 2014, **53**, 1845–1848.

36 Q. Liu, Y. Huang, Z. Li, L. Li, Y. Zhao and M. Li, An Enzymatically Gated Catalytic Hairpin Assembly Delivered by Lipid Nanoparticles for the Tumor-Specific Activation of Signal Amplification in miRNA Imaging, *Angew. Chem., Int. Ed.*, 2022, **61**, e202214230.

37 Y. Zhang, C. Yang, J. He, S. Zuo, X. Shang, J. Gao, R. Yuan and W. Xu, Target DNA-Activating Proximity-Localized Catalytic Hairpin Assembly Enables Forming Split-DNA Ag Nanoclusters for Robust and Sensitive Fluorescence Biosensing, *Anal. Chem.*, 2022, **94**, 14947–14955.

38 Z. Weng, H. Yu, W. Luo, Y. Guo, Q. Liu, L. Zhang, Z. Zhang, T. Wang, L. Dai, X. Zhou, X. Han, L. Wang, J. Li, Y. Yang and G. Xie, Cooperative Branch Migration: A Mechanism for Flexible Control of DNA Strand Displacement, *ACS Nano*, 2022, **16**, 3135–3144.

39 L. Deng, Y. Wu, S. Xu, Y. Tang, X. Zhang and P. Wu, Improving the Signal-to-Background Ratio during Catalytic Hairpin Assembly through Both-End-Blocked DNAzyme, *ACS Sens.*, 2018, **3**, 1190–1195.

40 L. Zhao, Y. Song and H. Xu, Catalytic hairpin self-assembly for biosensing: classification, influencing factors, and applications, *TrAC, Trends Anal. Chem.*, 2024, **171**, 117508.

41 J. Mehta, B. Van Dorst, E. Rouah-Martin, W. Herrebout, M.-L. Scippo, R. Blust and J. Robbens, In vitro selection and characterization of DNA aptamers recognizing chloramphenicol, *J. Biotechnol.*, 2011, **155**, 361–369.

42 Y. Zhang, W.-G. Yang, M.-L. Su, B.-W. Wang, R. Yuan and W.-B. Liang, A reagent-based label free electrochemiluminescence biosensor for ultrasensitive quantification of low-abundant chloramphenicol, *Microchem. J.*, 2024, **198**, 110124.

43 T. Mayer, L. Oesinghaus and F. C. Simmel, Toehold-Mediated Strand Displacement in Random Sequence Pools, *J. Am. Chem. Soc.*, 2023, **145**, 634–644.

44 N. Srinivas, T. E. Ouldridge, P. Šulc, J. M. Schaeffer, B. Yurke, A. A. Louis, J. P. K. Doye and E. Winfree, On the biophysics and kinetics of toehold-mediated DNA strand displacement, *Nucleic Acids Res.*, 2013, **41**, 10641–10658.